Use of Seeds to Control Precipitation of Calcium Carbonate and Determination of Seed Nature

ARTICLE *in* LANGMUIR · FEBRUARY 2005

Impact Factor: 4.46 · DOI: 10.1021/la048525i · Source: PubMed

5 AUTHORS, INCLUDING:

Marcel Donnet
Electro Medical Systems
24 PUBLICATIONS **216** CITATIONS
SEE PROFILE

Paul Bowen
École Polytechnique Fédérale de Lausanne
173 PUBLICATIONS **2,632** CITATIONS
SEE PROFILE

Nathalie Jongen
École Polytechnique Fédérale de Lausanne
34 PUBLICATIONS **453** CITATIONS
SEE PROFILE

Heiri Hofmann
École Polytechnique Fédérale de Lausanne
239 PUBLICATIONS **4,387** CITATIONS
SEE PROFILE

Use of Seeds to Control Precipitation of Calcium Carbonate and Determination of Seed Nature

Marcel Donnet, Paul Bowen,* Nathalie Jongen, Jacques Lemaître, and Heinrich Hofmann

Ecole Polytechnique Fédérale de Lausanne (EPFL), Powder Technology Laboratory, Materials Institute, CH-1015 Lausanne, Switzerland

Received June 15, 2004. In Final Form: September 30, 2004

Understanding and controlling precipitation reactions is a major challenge for industrial crystallization. Calcium carbonate is a widely studied system: more than 3000 papers have been devoted to the subject over the past 10 years. The first step of the precipitation of calcium carbonate, from relatively concentrated solutions (0.01 mol/L), involves the formation of an initial gel phase which later transforms into calcite, vaterite, or a mixture of both phases. Our work aimed at controlling this first step. Nanosized seeds (8 nm), formed in situ, were used in order to control the often chaotic nucleation step which normally leads to poor phase selection and broad particle size distributions. Seeding has often been used to avoid spontaneous nucleation in metastable solutions for growth mechanism investigations of single-crystal calcium carbonate. Here the ability of a seeding method to control the precipitation reaction evolution even in the case of high supersaturation is demonstrated. The seeds and the presence of a polymeric additive (poly(acrylic acid)) allow the control of the precipitated polymorph and the specific surface area, while maintaining a narrow particle size distribution in the submicron range. Direct characterization methods did not succeed in identifying these nanoseeds; indirect methods using solubility calculations are used to demonstrate their existence and quantify size and number density of the nanosized seeds.

1. Introduction

The calcium carbonate system is a widely studied system with more than 3000 papers devoted to this system over the last 10 years. Among these papers, many are devoted to the chemical synthesis of different morphologies and particle sizes of calcium carbonate in its different crystallographic forms; calcite, vaterite, and aragonite. Calcium carbonate of a particular size, shape, and crystallographic phase is used in various commercial applications such as in paper coatings or as fillers for rubber materials. Modification of calcium carbonate powder characteristics is generally obtained by the use of additives such as sulfate ions,[1,2] carboxylic acids,[3] phosphates,[4] or various polymers,[5] while carrying out the reaction without any additive leads to difficulties in controlling the shape and the precipitated crystallographic form.[29]

To control the precipitation reaction, the nucleation and growth steps must be mastered. The nucleation step is especially important in precipitation reactions. The rate of nucleation and the duration of the nucleation process have a direct influence on the final particle size, the size distribution, and to some degree the growth mechanism.[30] Unfortunately, this step is the most difficult to control, especially at high concentrations where high supersaturations induce high nucleation rates and sometimes the precipitation of metastables phases which can consequently transform into the thermodynamically stable phase. In the case of calcium carbonate which has a low solubility product, relatively high supersaturations are created at solution concentrations of 0.01 M, where an initial metastable gel phase is observed before transformation into a crystalline material.[6−10] Recently, new analytical methods such as fast drying,[11] cryogenic transmission electron microscopy (cryo-TEM),[11] or X-ray microscopy[13] have allowed the observation of the initial gel phase in the precipitation pathway towards a crystalline calcium carbonate. This gel is composed of small particles around 30 nm randomly agglomerated.[11] This precursor seems to be stabilized by different additives such as phosphates[31] or block copolymers.[11] The duration of stabilization can be from 5 to 90 min before further transformation into a recoverable powder. Unfortunately, these observation methods for the gel stage were not able to determine the crystallographic phase of these nanoparticles (hydrate or anhydrate).

The use of seeds can help control the apparently "chaotic" nucleation step. In most previous studies, the seeding method has been used to prevent spontaneous nucleation in metastable solutions (≈0.002 M) for growth mechanism studies of large (>50 μm) calcium carbonate crystals.[14−17]

* To whom correspondence should be addressed. Tel: +41 21 693 49 07. Fax: +41 21 693 30 89. E-mail: Paul.Bowen@epfl.ch.

(1) Tracy, S. L.; Francois, C. J. P.; Jennings, H. M. *J. Cryst. Growth* **1998**, *193*, 374.
(2) Tracy, S. L.; Williams, D. A.; Jennings, H. M. *J. Cryst. Growth* **1998**, *193*, 382.
(3) Wada, N.; Yamashita, K.; Umegaki, T. *J. Colloid Interface Sci*. **1999**, *212*, 357.
(4) Didymus, J. M.; Oliver, P.; Mann, S.; DeVries, A. L.; Hauschka, P. V.; Westbroek, P. *J. Chem. Soc., Faraday Trans.* **1993**, *89−15*, 2891.
(5) Verdoes, D.; Kashchiev, D.; Van Rosmalen, G. M. *J. Cryst. Growth* **1992**, *118*, 401.
(6) Kamiya, K.; Sakka, S.; Terada, K. *Mater. Res. Bull.* **1977**, *12*, 1095.
(7) Kind, M. *Industrial Crystallization 99*; IChemE: Cambridge, 1999.
(8) Gösele, W.; Egel-Hess, W.; Windmantel, K.; Faulhaber, F. R.; Mersmann, A. *Chem. Ing. Tech.* **1990**, *62−7*, 544.
(9) Houstomsky, J.; Jones, A. G. *J. Phys. D*: *Appl. Phys*. **1991**, *24*, 165.
(10) Kitamura, M. *J. Colloid Interface Sci.* **2001**, *236*, 318.
(11) Cölfen, H.; Qi, L. *Chem.−Eur. J.* **2001**, *7−1*, 106.
(12) Rieger, J.; Hdicke, E.; Rau, I. U.; Boeckh, D. *Tenside, Surfactants, Deterg.* **1997**, *34−6*, 430.
(13) Rieger, J.; Thieme, J.; Schmidt, C. *Langmuir* **2000**, *16−22*, 8300.
(14) Gomez-Morales, J.; Torrent-Burgues, J.; Lopez-Macipe, A.; Rodriguez-Clemente, R. *J. Cryst. Growth* **1996**, *166*, 1020.
(15) Takasaki, S.; Parsiegla, K. I.; Katz, J. L. *J. Cryst. Growth* **1994**, *143*, 261.
(16) Teng, H. H.; Dove, P. M.; Orme, C. A.; Deyoreo, J. J. *Science* **1998**, *282*, 724.

10.1021/la048525i CCC: $30.25
Published on Web 11/25/2004

Few structured experiments have been carried out on the seeding of high-concentration solutions of calcium carbonate which produce micron-sized particles. The aim of the present study is to show the ability of a seeding method to control the precipitation reaction evolution even if supersaturations are high. This has been carried out using seed dispersions prepared with the aid of a specific polymeric additive, poly(acrylic acid), for the precipitation reaction between aqueous solutions of calcium nitrate and potassium carbonate. The method for producing and characterizing the "nanoseeds" (<20 nm) used will also be described. The seeds were not directly observable by traditional methods such as transmission electron microscopy (TEM) or photon correlation spectroscopy (PCS). Their size and nature were determined by a combination of solubility and interfacial energy considerations using the Kelvin equation. The nature of the seed source used, calcite or vaterite, determined the nature of the seeds and the final precipitated phase. The approach provides a route for the precipitation of controlled calcite particles with specific surface areas of between 5 and 35 m^2/g with relatively constant particle sizes around 1 micron. The morphology and the specific surface areas of the particles are also influenced by the precipitation conditions and can be varied in a controlled manner.

2. Materials and Methods

The reaction studied is the precipitation that results from the mixing of calcium nitrate and potassium carbonate aqueous solutions (eq 1).

$$Ca(NO_3)_2 + K_2CO_3 \xrightarrow[H_2O]{} CaCO_3(s) + 2K^+ + 2NO_3^- \quad (1)$$

The calcium nitrate reactant is prepared by dilution from a stock solution (Fluka, calcium nitrate tetrahydrate, p.a., 99%, no. 21197), which is titrated by EDTA (ethylenediaminotetraacetic acid). The water used for the stock solution preparation and for the reaction was ultrapure water (0.055 μS/cm with membrane filtration at 0.2 μm).

The potassium carbonate reactant was prepared just before performing the reaction by dissolving the powder (Merck, potassium carbonate, p.a. 99.9%, no. 1.04928) in ultrapure water.[18] Acid−base titration allows us to compute the exact concentration of the reactant. This procedure is used to minimize the amount of dissolved carbonic gas in the reactant solution so that its concentration does not exceed 10^{-5} M.

A polymeric additive is used to produce the seeds, poly(acrylic acid) (PAA 2000, Acros, 18499). A stock solution of about 2 wt % is prepared, and acid−base titrations indicate that a molecule of the average molecular weight, Mw = 2000, would contain 22 equivalent acid groups. The PAA solution is then added to the potassium carbonate reactant to give PAA concentrations of between 0.001 and 0.01 wt %.

Commercial powders were used either as seeds or seed sources or to calibrate the Ca specific electrodes. The commercial powders used were a high specific surface area calcite (Calofort U, Speciality Minerals, S_{BET} = 21 m^2/g, Figure 1) and a low specific surface area calcite (Fluka 21060, S_{BET} < 1 m^2/g).

The seed suspensions were prepared as follows: a seed source (a calcium carbonate powder with high specific surface area) is suspended in the potassium carbonate reactant (0.044 M) which already contains PAA (0.01−0.001 wt %). Five minutes of ultrasonic treatment (bath) is applied to this suspension before filtering the seed source through a 0.2 μm membrane to remove the bigger particles. The resulting filtrate is transparent and contains only the sub-200-nm seeds (the nature of which will be described and discussed later).

(17) Kavanagh, A. M.; Rayment, T.; Price, T. J. *J. Chem. Soc., Faraday Trans.* **1990**, *86−6*, 965.
(18) Kralj, D.; Brecevic, L.; Nielsen, A. E. *J. Cryst. Growth* **1990**, *104*, 793.

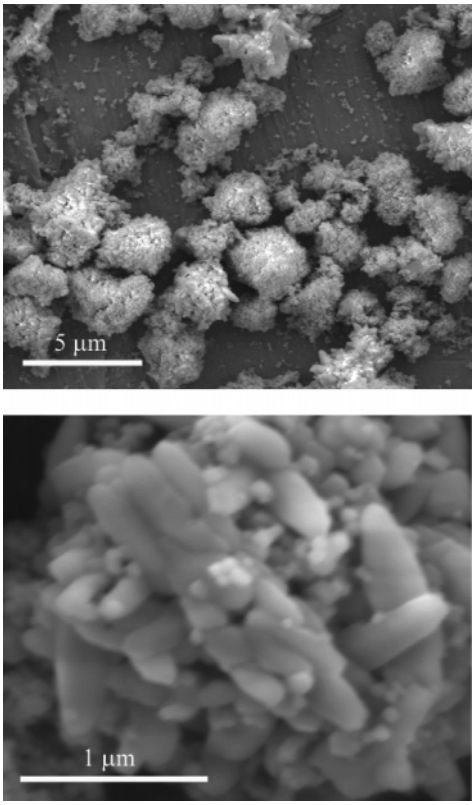

Figure 1. Scanning electron micrographs showing the morphology and microstructure of the Calofort U commercial calcite powder with S_{BET} = 21 m^2/g.

Table 1. Experimental Conditions after Mixing of the Reactants[a]

parameter	value	parameter	value
$\{Ca^{2+}\}_{t=0}$ (M)	0.02	supersaturation ($S = P_S/K_S$)	48
CO_3/Ca	1.1	temperature (°C)	25

[a] Supersaturation S was calculated using the activity product of the calcium and carbonate ion divided by the solubility product. Correction for different complex formation is also taken into account to determine the right amount of calcium and carbonate ions.

Precipitation reactions were carried out in a 20 mL fed-batch reactor. Good mixing was achieved by impinging the two reactants (parallel jets with a velocity of 127 cm/s) on the bottom of the reactor vessel. The filling up of the reactor takes 5 s, and no effects of this filling up time were observed on the resulting precipitates because the mixing takes place directly when the two reactants hit the bottom. The effective mixing time was estimated at around 50−100 ms by comparison with results obtained using a micromixer. Therefore the reactants can be assumed to be well mixed for the analytical measurements that followed the initial injection. In-line filtration (0.45 μm) was carried out just before the injection pistons to eliminate residual dust which may influence the nucleation step. After injection, the reaction mixture was aged without any agitation.

Experimental concentrations were chosen so that the reaction starts with a gel phase[7,8] and a slight excess of carbonate compared to the stoichiometry of 1 for $CaCO_3$ (Table 1).

The particle size distribution of the resulting powders was measured by laser diffraction (Malvern Mastersizer S, ρ = 2.71 g/cm^3, n = 1.596, i = 0.10, in water). The specific surface areas for the various precipitates, S_{BET} (m^2/g), were obtained by nitrogen adsorption (Brunauer−Emmett−Teller (BET) model, Gemini 2375, Micromeritics), which allows us to estimate the size of the primary particles, d_{BET} (μm), assuming spherical monodisperse particles (eq 2).

$$d_{BET} = \frac{6}{S_{BET}\rho} \quad (2)$$

Samples were observed by scanning electron microscopy (SEM, Philips XL-30 FEG) and by transmission electron microscopy (Philips EM 430). Crystallographic phase contents were monitored using X-ray diffraction (XRD, Kristalloflex 805, Siemens, using a copper electrode with $\lambda_{X1} = 1.540\ 60$ Å and $\lambda_{X2} = 1.544\ 43$ Å). When the precipitated phase in the following text is described as pure calcite, no reflections other than calcite were observed. The impurities or secondary phases are therefore below the XRD detection limit at around 1−2 wt %. The XRD peak broadening allows us to determine the size of the primary crystallite using the Scherer equation (eq 3).[19] The instrumental peak broadening was determined using a calcium carbonate with a large crystal size (>1 μm, Fluka).

$$d_{XRD} = \frac{K\lambda_X}{\beta_{Xp}\cos(\theta)} \tag{3}$$

where K is equal to 1, λ_X is the X-ray wavelength, and β is the peak width at half intensity, calculated using $\beta = \sqrt{(\beta^2_{sample} - \beta^2_{Fluka})}$.

The total calcium concentration, in the different filtrates described later, was analyzed using inductively coupled plasma spectrometry (ICP-AES, Perkin Elmer, Plasma 2000 software). Solid residual particles in the filtrate are also taken into account using this method. Solution pHs and free calcium activity (ions in solution) were recorded with pH and Ca specific electrodes (pH, Orion 8115BN; Ca, Orion 9700BN).

2.1. Solubility Calculations. Results are analyzed using solubility calculations as described by Donnet.[33,34] All equilibrium constants are also solved simultaneously considering the activity of each species in solution.

Concentrations are then obtained using the Debye−Hückel definition of the activity coefficient.[24,25] Additional corrections are made to the solubility constants as a function of the particle size using the Kelvin law for spherical particles (eq 4):[33,34]

$$\ln\left(\frac{K_{sr}}{K_s}\right) = \frac{4\gamma}{r}\frac{V_m}{RT} \tag{4}$$

where K_{sr} is the solubility constant of particles with r radius, K_s is the solubility constant for infinite crystals, γ is the crystal−solution interfacial tension, r is the radius of the particle, V_m is the molar volume, R is the gas constant, and T is the temperature in kelvin.

3. Results

3.1. Characterization of the Seed Suspensions. Direct observation methods such as cryogenic-TEM or PCS did not allow us to observe any particles in the seed suspensions. The observation of the seeds was rendered difficult due to several factors. The seeds are dispersed in a solution containing around 100× the quantity of calcium in the seeds themselves (see data in Tables 3−8 discussed later). On drying such a suspension, a significant quantity of a "secondary" precipitate is formed, making it difficult to identify the original seeds. We tried to overcome this by using cryo-TEM where liquid ethane is used to freeze a suspension, the water remaining amorphous. Again, even using this method it was not possible to distinguish "impurities" from seeds. This was complicated by the fact that elemental analysis could not be carried out because of the beam sensitivity of the amorphous water film. When using the seed suspension in precipitation experiments, marked effects of particle size and morphology were observed. Precipitation reactions without using the seed suspension produce final results which are chaotic in phase composition (variable amounts of vaterite and calcite) with large particle diameters ($d_{v50} = 12$ μm) Figure 2a. When using identical experimental procedures and solution concentrations, particle size distributions (PSDs) were very irreproducible.

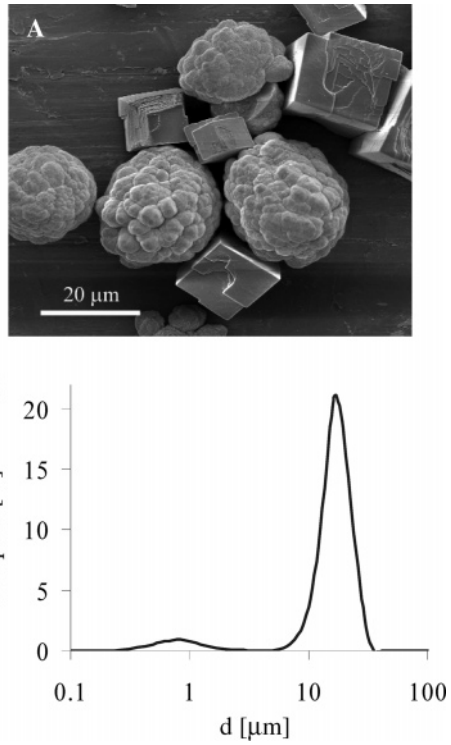

Figure 2. Typical (A) morphologies and (B) particle size distributions of mixed calcite (cubes) and vaterite (spheres) precipitates obtained in the absence of seeds.

Using a seed suspension (source: Calofort U, for example, 5.2 mg/L) in combination with PAA (0.01 wt %), the morphology is a well-defined rice shape, the only crystallographic phase detected by XRD is calcite, the particle size is less than 10 μm, and the size distribution is narrow. The breadth of a distribution can be described by the span defined as $d_{v90} - d_{v10}/d_{v50} \cong 1$ (Figure 3).

To clarify the effect of these sub-200-nm nonobservable "seeds", an experiment was carried out with the powder shown in Figure 3 as the seed source. The seed suspension used 0.5 g/L of the powder with 0.001 wt % of PAA. The seed source was not removed from the seed suspension by filtration but was used directly in the reactant solution for the experiment. Observation of the precipitation product, pure calcite, in the SEM shows two populations of particles, a submicron population and particles around 2−3 microns (Figure 4).

The bimodal PSD observed in Figure 4 suggests the presence of two seed types: the rice-shaped particles themselves and the nonobservable nanoseeds. The shift of the second PSD mode from 2 to 4 μm is indicative of growth of the rice particle seed source.

Direct observation methods, as mentioned above, were not able to demonstrate the existence of a solid phase that we believe acts as seeds. To support our hypothesis of a "nonobservable" solid phase, seed sources of vaterite and aragonite as well as calcite were investigated. Seed sources of all three phases were produced by dispersion in 0.01 wt

(19) Klug, H. P.; Alexander, L. E. *X-ray Diffraction Procedures*, 2nd ed.; Wiley-Interscience: New York, 1974; pp 687−707.
(20) Kotrly, S.; Sucha, L. *Handbook of Chemical Equilibria in Analytical Chemistry*; Ellis Horwood: Chichester, 1985.
(21) Plummer, L. N.; Busenberg, E. *Geochim. Cosmochim. Acta* **1982**, *46*, 1011.
(22) Bischoff, J. L.; Fitzpatrick, J. A.; Rosenbauer, R. J. *J. Cryst. Growth* **1993**, *101*, 21.
(23) Geffroy, C.; Foissy, A.; Persello, J.; Cabane, B. *J. Colloid Interface Sci.* **1999**, *211*, 45.
(24) Rubattel, S.; Lemaître, J.; Bowen, P.; Ring, T. A. *J. Cryst. Growth* **1994**, *135*, 135.
(25) Vereecke, G.; Lemaître, J. *J. Cryst. Growth* **1990**, *104*, 820.

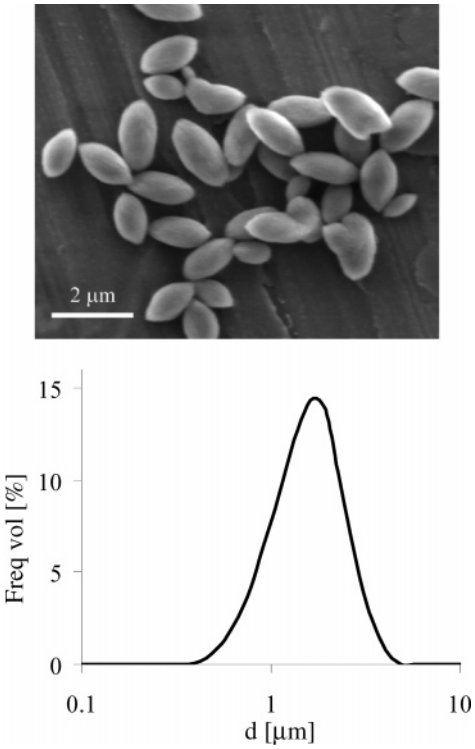

Figure 3. Morphology and particle size distribution of the resulting powder using a seed source (5.2 mg/L Calofort U) to generate nanoseeds in order to control the reaction.

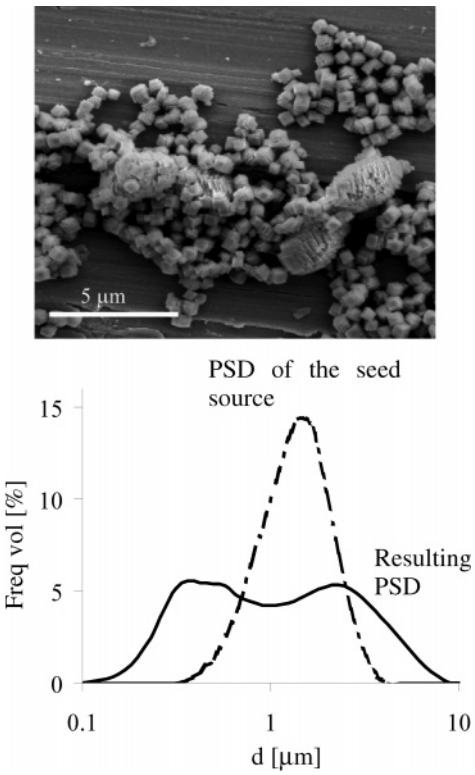

Figure 4. Resulting powder obtained without removing the seed source in the presence of 0.001 wt % PAA. The bimodal PSD suggests growth on the seed source as well as growth on the nanoseeds.

% PAA solutions as described earlier. In each case, the micron-sized seed source particles were removed by filtration at 200 nm. XRD analysis of the resulting precipitates showed a pure phase of the same nature as the seeds for the calcite seed solution. For the vaterite seed source, which was 95% vaterite and 5% calcite, the precipitate was predominantly vaterite (90%) with some calcite (10%) formed. The aragonite seed source was relatively impure at around 60% aragonite and 40% calcite. The resulting powder from this "aragonite" seed source was calcite. The morphologies of the seed source and precipitated product for these three seed source experiments are presented in Figure 5. We observe that the rice grain morphology of the calcite and spherical shape of the vaterite are conserved. The aragonite seed source produces a different morphology from the original needles, showing a rounded cuboid morphology. The origin of this striking behavior with the aragonite system remains for the moment unexplained; presumably the nature of the "as of yet" uncharacterized seeds is different from that of the pure calcite system.

The memory effect of the seed source crystallography demonstrated by these experiments (Figure 5) adds weight to our belief that a solid seed phase exists in the seed solutions but is too small and too dilute to be observed. Without the seed source, precipitates with irreproducible and varied amounts of calcite and vaterite are produced. Filtration of the seed source a second time through a 20 nm filter does not reduce its effect on the calcium carbonate precipitation. Precipitates of pure calcite (>98%) of a similar size (d_{v50} = 650 nm) and specific surface area (34 m^2/g) as the rice grain shaped seed source are produced. This indicates that the seeds are smaller than 20 nm. This led us to speculate about the possible role of PAA as a nucleation agent, but if PAA alone is used random uncontrollable results are obtained with respect to both particle size and phase composition. Further indirect evidence of the existence of the seeds is presented in section 4.5.

3.2. Role of PAA. The phase selectivity and size control of the precipitates are only observed if PAA is combined with a seed source. If only PAA is present in the solution, no reaction control effects are observed. Consequently, the PAA seems necessary to generate and stabilize the nanoseeds. To better understand the role of PAA, a series of experiments were carried out whereby the PAA concentration was varied while keeping the other reaction parameters constant. The amount of PAA was increased in four steps from 0.0010 to 0.0033, 0.0066, and 0.0100 wt % The seed source used was the rice-shaped particles of Figure 3 (0.47 g/L). The seed source was removed from the reactant stream before the reaction by filtration at 200 nm. The resulting powders show differences in their morphology (Figure 6) and their specific surface area (Table 2). The primary crystallite size from both the S_{BET} and XRD line broadening as well as the particle size from laser diffraction are presented for each powder in Table 2.

There is an increase in specific surface area and a decrease in the crystallite size (primary particles) with increasing PAA concentration. The particle size measured by laser diffraction however remains similar, between 500 and 800 nm. These results indicate that the particles observed by SEM and laser diffraction are agglomerates of smaller primary particles. This is confirmed for the 0.01% PAA powder from nitrogen adsorption−desorption isotherms which show significant open porosity of 0.05 cm^3/g with pore sizes around 10 nm.

3.3. Complementary Characterization: In Search of Nanoseeds. Despite the controlling effect of the seed solution even when filtered at 20 nm, no direct observation method (e.g., TEM, PCS) succeeded in showing the existence of these seeds; indirect methods using solubility measurements and TEM observations of the seed source

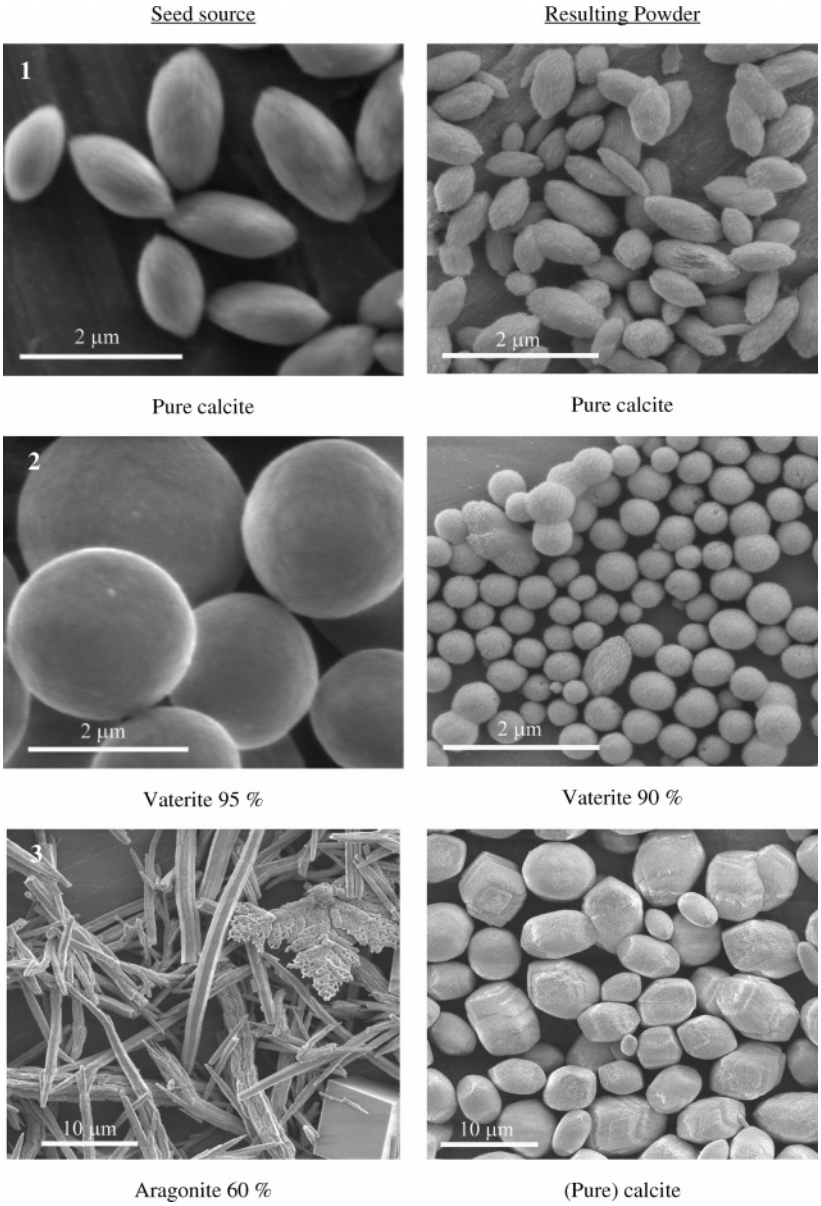

Figure 5. Seed source and resulting powder: (1) seed source is calcite, resulting powder is calcite also; (2) seed source is vaterite, resulting powder is mainly vaterite; (3) seed source is mainly aragonite, resulting powder is calcite.

will be presented that help elucidate the nature and size of the seeds. TEM (Figure 3) of the seed source shows a surface roughness of about 10 nm (Figure 7) and suggests that the external surface is composed of 10 nm crystallites.

Therefore it seems possible that PAA allows the erosion and dispersion of these 10 nm surface crystallites observed in the TEM. This may be likened to the production of secondary nuclei by surface erosion and is supported by the fact that the "seed source" loses its seeding capacity after it has been used 4−5 times. These seeds are assumed to be colloidally stabilized by the PAA and will be in chemical equilibrium with the solution phase governed by their size and interfacial energy as predicted by the Kelvin law. Therefore to determine the seed size and number density from the Kelvin equation the following data need to be evaluated: (1) the exact repartition of the total calcium in the system (solid phase, complexes (including PAA), and free calcium in solution); (2) the calcium−solution interfacial tension, which may be evaluated using the Kelvin law and a calcite powder of known specific surface area.

Calcium can be found in the solution in the form of various complexes or solid phases; the quantity of each will depend on their equilibrium constants and the solution composition.[33,34] Most of these species and their thermodynamic data are well documented in the chemistry literature, but the PAA−calcium constant is not known and needs to be evaluated. Measurements were carried out to determine this constant and the repartition of the calcium in the seed suspensions. From these data, solubility measurements can be correlated to the size of the particles using the Kelvin equation. The total amount of calcium can be determined by ICP (solid-phase complexes and Ca^{2+}) and Ca^{2+} in solution using a calcium specific electrode.

(i) Measurements To Determine the PAA−Calcium Complexation Constant. Measurements were carried out using calcium nitrate solutions with PAA at basic pH (KOH $= 2 \times 10^{-3}$ M). Calcium activity was then measured with the calcium specific electrode for several PAA concentrations (Table 3).

Measurements were stable during at least 1 h. The error in the Ca activity considers only the electrode precision.

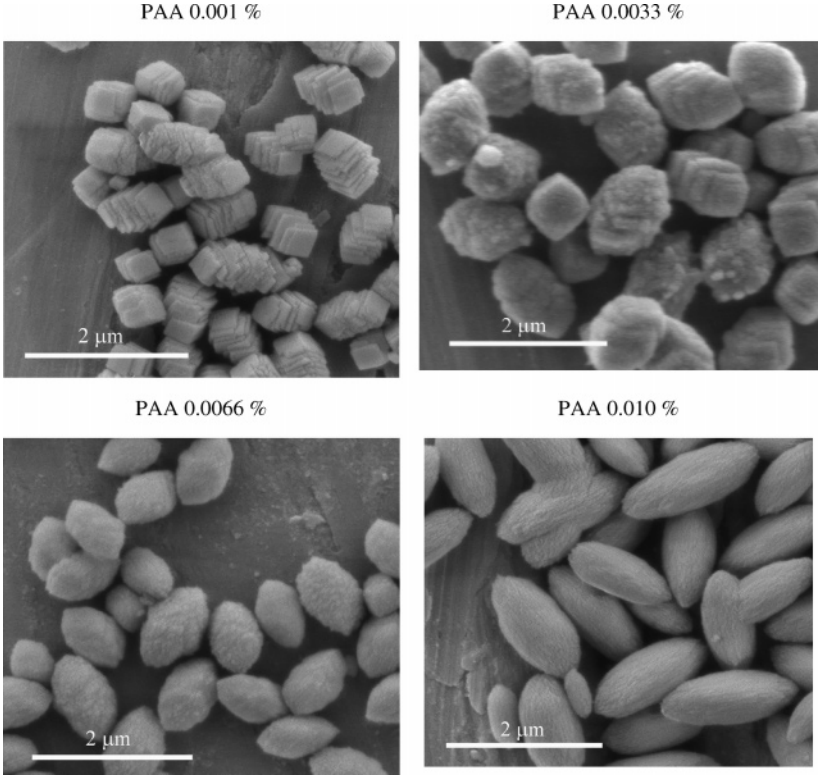

Figure 6. Morphology of the powder as a function of the added PAA amount.

Table 2. Specific Surface Area and Its Corresponding Primary Particle Size Compared with Crystallite Size and Agglomerate Size for Different PAA Concentrations

PAA concn [wt %]	S_{BET} [m²/g]	d_{BET} [nm]	d_{XRD} [nm]	$d_{v50\ Malvern}$ [nm]
0.0010	6.7	330 ± 40	102 ± 20	500 ± 50
0.0033	16.1	138 ± 10	110 ± 20	850 ± 50
0.0066	25.9	85 ± 4	85 ± 7	570 ± 50
0.0100	34.2	65 ± 3	67 ± 6	650 ± 50

Table 3. Calcium Activity Measurements as a Function of the PAA Content in Basic Media (KOH = 2 × 10^{-3} M)

PAA [%] (mass)	{Ca} [mol/L]	T [°C]	pH	a(Ca) [mol/L] (×10^{-4})
0	10^{-3}	24.4	11.33	7.20 ± 0.03 (reference)
0.002	10^{-3}	25.0	11.25	6.45 ± 0.03
0.010	10^{-3}	24.7	10.97	4.52 ± 0.03
0.020	10^{-3}	24.7	6.59	2.67 ± 0.03

(ii) Measurements Carried Out on the Experimental Filtrate To Determine the Repartition of the Ca. Two standards, solutions in equilibrium with low specific surface area calcite (Fluka, $S_{BET} \cong 1 m^2/g$), were used to calibrate the Ca electrode (standards 1 and 2, Table 4). Control measurements (controls 1 and 2, Table 4) were then made on solutions in equilibrium with high specific surface area calcite (Calofort U, $S_{BET} = 21 m^2/g$). Finally, reactants as prepared according to the seed source preparation protocol were measured (PAA = 0.020% and PAA = 0.002%, Table 4). The seed source was the rice-shaped particles (Figure 3) at 0.47 g/L, which were removed by filtration at 20 nm. Table 4 reports the measured values taking into account the measurement variation during 1 h.

We now have the data necessary for the evaluation of (i) the PAA complexation constant, (ii) the interfacial tension of calcite with respect to the solution composition (measured calcium activity), (iii) the size of the seeds, and finally (iv) the number density of the seeds in a given seed source suspension.

4. Determination of the Size and Number Density of the Seeds

We hypothesize that the nanoseeds are produced by erosion of the seed source surface by dissolution of necks between the surface particles and the core and remain dispersed as a suspension by the stabilizing effect of the PAA as illustrated schematically in Figure 8. The aim of our discussion is neither this erosion mechanism nor the colloidal stability of the nanoseeds but the determination of the existence, the size, and the number density of the seeds using the Kelvin law from the data collected in the previous sections.

4.1. Determination of the PAA−Ca Complexation Constant. Calculation of a complexation constant for a polyelectrolyte such as PAA may be simplified by using the equivalent number of dicarboxylate (glutarate) molecules that are needed to represent a PAA molecule. We consider the dicarboxylate as the primary functional group because it should have a better complexation behavior with respect to calcium as opposed to monocarboxylate groups[23,26,27] which complex calcium to a much lesser degree (Figure 9).

According to pH titration of the PAA, the number of dicarboxylate groups for the 2000 average Mw of the PAA used is 11. To refine our solubility calculations, we have to evaluate the calcium complexation constant for these dicarboxylate functionalities inside the PAA, considering for the apparent constant each dicarboxylate as an independent entity.

From the knowledge of the starting Ca concentration in a calcium nitrate solution, the total Ca is known. The calcium activity for the $CaNO_3$ solution is measured, and then the difference between the Ca activity measured in the presence of different PAA concentrations can be

(26) Compton, R. G.; Brown, C. A. *J. Colloid Interface Sci.* **1995**, *170*, 586.
(27) Mann, S.; Didymus, J. M.; Sanderson, N. P.; Heywood, B. R.; Samper, E. J. A. *J. Chem. Soc., Faraday Trans.* **1990**, *86−10*, 1873.

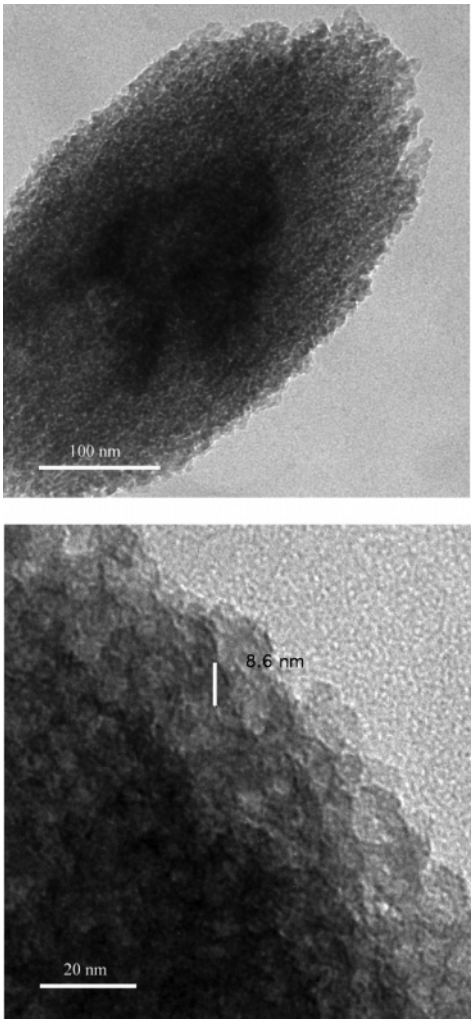

Figure 7. TEM observation of a seed source particle (Figure 3).

attributed to complexation with PAA (Table 5). The various other complexes[33,34] have been taken into account, and the expected pH can be calculated. Comparing the calculated pH with that measured confirms the correct attribution of the Ca to the various complexes in the equilibria calculations.

This leads to an apparent complexation constant of one bicarboxylate group of the PAA chain as

$$\log(K_{\mathrm{Glu3}}) = 4.0 \pm 0.15$$

4.2. Interfacial Tension of Calcite. In the Kelvin law (eq 4), there are four important parameters: the solubility constants for an infinite crystal and particles of size r, K_s and K_{sr}, respectively; the size of the primary particles; and the interfacial tension. Using the low surface area pure calcite (standards 1 and 2, Table 4), K_s can be determined. Knowing the size of the primary particle through specific surface area measurements, which is the case for the control 1 and control 2 experiments using the Calofort U calcite of Table 4, it is then possible to determine, using the free calcium in solution measurement, the specific calcite−solution interfacial tension for these conditions (Table 6).

The potassium carbonate concentration of the control 1 experiment is exactly the same as used for the reactant solutions in the precipitation experiments so that we can consider this interfacial tension measurement for further calculations. The difference between the two calculated interfacial tensions can be explained according to the Grahame experiments:[32] the interfacial tension is maximum when the surface potential is minimum. In the control 1 experiment, the potassium carbonate concentration is high so that we are very far from the isoelectric point and the surface potential should be high according to the Nernst law.[33,34] In the control 2 experiment, the potassium carbonate concentration is low so that we approach more closely the isoelectric point and, as a

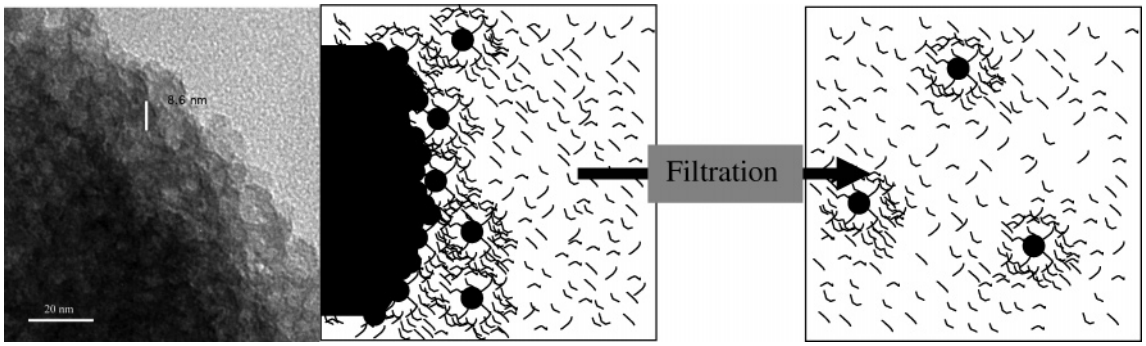

Figure 8. Schematic representation of the surface erosion mechanism which produces the nanoseeds.

Table 4. Total Calcium Concentration and Activity of the Free Calcium in Standard, Control, and Seed Solutions

sample	$[CO_3^{2-}]$	powder	pH	T [°C]	$\{Ca\}_{ICP}$ [mol/L] ($\times 10^{-6}$)	$a(Ca)_{free}$ [mol/L] ($\times 10^{-7}$)
standard 1	0.0403	Fluka	11.20	22.0	6.33 ± 0.05	3.53 ± 0.03 (ref)
standard 2	0.00403	Fluka	10.87	22.0	8.03 ± 0.05	17.0 ± 0.5 (ref)
control 1	0.0403	Calofort	11.17	22.0		3.75 ± 0.05
control 2	0.00403	Calofort	10.83	22.2		19.8 ± 0.7
PAA = 0.020%	0.0403	Filtred rice	11.02	22.7	74.2 ± 0.5	7.7 ± 0.2
PAA = 0.002%	0.0403	Filtred rice	11.18	23.4	35.1 ± 0.5	7.1 ± 0.5

Table 5. Determination of the Apparent Complexation Constant of the Dicarboxylate (Glutarate) Function of the PAA Chain by Adjusting the Calculated Calcium Activity to the Experimental Value[a]

$PAA\ [\%]_{mass}$	$pH_{measured}$	$pH_{calculated}$	$a(Ca)_{measured}$ [mol/L] × 10^{-4}	$a(Ca)_{calculated}$ [mol/L] × 10^{-4}	$\log(K_{Glu})$	[CaGlu]/{Ca} [%]
0.010	10.97	10.93	4.52	4.52	3.89	43
0.020	6.59	5.76	2.67	2.67	4.08	66

[a] The proportion of calcium present in the complex form is also reported in this table.

Table 6. Determination of the Calcite−Solution Interfacial Tension Using the Calcium Activity Measurement of a Solution in Equilibrium with Calofort U Calcite

experience	$pH_{measured}$	pH_{calc}	$a(Ca)_{measured}$ [mol/L] ($\times 10^{-7}$)	$S_{BET\ Calorfort}$ [m^2/g]	d_{BET} [nm]	γ_{calc} [mN/m]
control 1	11.17	11.23	3.75 ± 0.05	21	105	46 ± 7
control 2	10.83	10.89	19.8 ± 0.7	21	105	135 ± 29

Table 7. Size of the Seeds Obtained by Adjusting the Calculated Calcium Activity to the Measured Calcium Activity (Table 4) at Constant Interfacial Tension

	$pH_{measured}$	pH_{calc}	γ [mN/m]	$a(Ca)_{calc}$ [mol/L] ($\times 10^{-7}$)	d_{seeds} [nm]
PAA = 0.02%	11.02	10.94	46 ± 7	7.7 ± 0.2	7.5 ± 1.4
PAA = 0.002%	11.18	11.19	46 ± 7	7.1 ± 0.5	7.7 ± 1.7

consequence, the surface tension is higher. Such effects are discussed in a previous paper.[34]

4.3. Size of the Seeds. To determine the size of the nanoseeds, we shall use the interfacial tension measured for calcite in the reactant solution (Table 6, control 1). The use of this value assumes that the PAA does not influence in an important manner the interfacial tension. If the PAA is adsorbed on the nanoseeds in a brushlike configuration with a low surface coverage, this assumption should be reasonable. This hypothesis is supported by the fact that both the seed particles in suspension and the PAA are negatively charged in the reactant solution. The particles because of the high excess of carbonate ions with regard to calcite and the PAA are totally dissociated at high pHs. Thus the PAA should adsorb in a brush type configuration with low surface coverage[28] as illustrated schematically in (Figure 10). This type of adsorption should

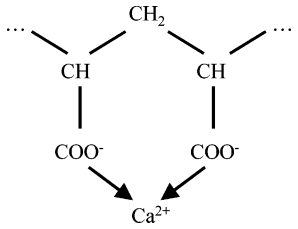

Figure 9. Schematic representation of the calcium complexation by the dicarboxylate group (glutaric acid) in the PAA.

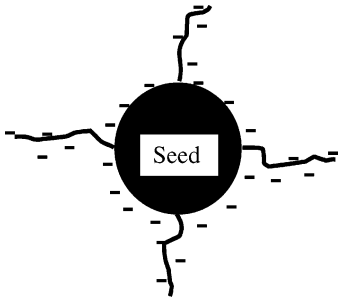

Figure 10. Schematic illustration of the probable brushlike adsorption configuration of negatively charged PAA on a negatively charged seed.

therefore not change significantly the interfacial tension.

The measured calcium activity of the seed suspensions (Table 4) allowed the calculation of the K_{sr} for the different conditions. Then, using the calcite−solution interfacial tension from the control 1 experiment, we can adjust a calculated calcium activity to the measured value (PAA = 0.02 and 0.002%, Table 4) by varying only the size of the seeds in equilibrium with this solution assuming monosized spherical seeds (Table 7).

As reported in Table 7, the calculated size of the seeds is very similar for the two PAA concentrations. This result is reasonable as the size of the seeds is determined by the seed source and not by the additive. This is also in agreement with the TEM observation of the seed source (Figure 7), which shows a surface roughness of about 9 nm.

For this determination, the PAA−calcium complexation constant does not play any important role because first the fraction of the calcium complexed by the PAA is low with regard to other complexes and second the error on this constant is reported on all different calcium complexes so that the real effect on the free calcium ion activity in solution is negligible.

4.4. Determination of the Number Density of the Seeds. The total calcium concentration determined by ICP provides us with the total amount of calcium in the filtered seed suspensions; this is assumed to be present in the form of solid particles in the form of our sub-20-nm seeds (Ca_{seeds}) and the various solution species and complexes including the PAA complex ($Ca_{calculated}$) (eq 5).

$$\{Ca\}_{ICP} = \{Ca\}_{calculated} + \{Ca\}_{seeds} \quad (5)$$

Using the amount of solid calcite (Ca_{seeds}) present in the seed suspension and from the size and hence mass of one seed, it is possible to determine the number density of seeds in the seed suspension (6, Table 1).

$$\text{no. of seeds} = \frac{\text{total mass of seeds}}{\text{mass of one seed}} \quad (6)$$

This determination is based on the assumption that seeds are composed of pure and dense calcite. For this calculation, the PAA−calcium complexation constant is important as it influences significantly the amount of the total calcium calculated in solution in equilibrium with solid particles.

Taking into account all errors in the various steps to the number density of the seeds, we get an error of ±50%. This precision is however good enough to show that the number of seeds generated varies with the PAA concentration.

Table 8 shows also that the number concentration of the seeds is very low, between 2 and 16 seeds per μm^3; such a low number density helps explain why the direct observation methods such as the PCS and TEM attempted did not succeed in revealing these particles. For example, in the TEM observations, this seed number density means that we have a probability to observe only one 8 nm particle in each hole of the TEM grid, which was too low to be observed.

4.5. Test of Hypothesis. So from our calcium activity measurements (Ca specific electrode), total calcium content (ICP measurements), and solubility calculations, we

(28) Pedersen, H. G.; Bergström, L. *J. Am. Ceram. Soc.* **1999**, *82*−*5*, 1137.
(29) Gomez-Morals, J.; Torrent-Burgues, J.; Rodriguez-Clemente R. *J. Cryst. Growth* **1996**, *169*, 331.
(30) Sathyagal, A. N.; McCormick, A. V. *AIChE J.* **1998**, *44* (10), 2312.
(31) Clarkson, J. R.; Price, T. J.; Adams, C. J. *J. Chem. Soc., Faraday Trans.* **1992**, *88* (2), 243.
(32) Grahame, D. C. *Chem. Rev.* **1947**, *41*, 441.
(33) Donnet, M. Ph.D. Thesis No. 2623, Ecole Polytechnique Fédérale de Lausanne (EPFL), Lausanne, 2002.
(34) Donnet, M.; Lemaître, J. *J. Colloid. Interface Sci.*, submitted.

Table 8. Determination of the Seed Number Density Based on Experimental Results

sample	$\{Ca\}_{ICP}$ [mol/L] ($\times 10^{-5}$)	d_{seeds} [nm]	pK_{Glu3}	$\{Ca\}_{calculated}$ [mol/L] ($\times 10^{-5}$)	no. of seeds/L ($\times 10^{15}$)
PAA = 0.02%	7.41 ± 0.05	7.5 ± 1.4	−4.0 ± 0.1	1.67 ± 0.09	11 ± 5
PAA = 0.002%	3.51 ± 0.05	7.7 ± 1.7	−4.0 ± 0.1	1.35 ± 0.07	4 ± 2

Table 9. Theoretical Particle Size Considering Only Growth of the Material (2 g/L) on the Seeds[a]

sample	d_{CAL} [nm]	d_{XRD} [nm]	d_{BET} [nm]
PAA_i 0.02%	65 ± 10	67 ± 6	63 ± 3
PAA_i 0.002%	91 ± 15	102 ± 20	330 ± 40

[a] For comparison purposes are presented the crystallite size measured by X-ray and the primary particle size measured by BET (Table 2).

have been able to calculate a size and number density of our "invisible" sub-20-nm seed. Now we return to the precipitation experiments where we have shown excellent phase and size control by the use of our assumed seed suspension (after filtering at 20 nm). From the total yield of the precipitation reaction (about 2 g/L), it is possible to estimate the maximum size of each particle generated only by growth on the seeds; i.e., there is no spontaneous calcite nucleation. We note that the seed number density is determined for the volume of the reactants before mixing, while the yield is determined for the reaction after mixing of the reactants (0.02% PAA in the seed-containing reactant and only 0.01% PAA in the precipitated product). In Table 9, the correlation of this calculated primary particle size, d_{CAL}, with the crystallite size from XRD line broadening (d_{XRD}) is very good indeed for the two extreme PAA concentrations. For the d_{BET} calculated from the specific surface area, the correlation is very good at high PAA concentrations but deviates significantly at the lower concentrations. This is believed to be due to a ripening effect for the low PAA concentrations as the initial stages were shown to be very similar in the cryo-TEM investigations and there is not enough PAA to totally cover the primary particle surface for the low PAA concentrations.[33]

The correlation between these three totally different measurement methods, especially in the case of the highest PAA amount, supports our use of solubility calculations to determine the size of nanoparticles which were not directly detectable but showed a coherent and reproducible effect on the precipitation of calcium carbonate in a well-mixed batch reactor.

5. Conclusions

We have investigated the precipitation of calcium carbonate from the mixing of potassium carbonate and calcium nitrate solutions at relatively high supersaturations ($S = 48$). At these supersaturations, the reaction passes initially via a gel phase and results in mixed precipitates of calcite and vaterite of several microns in size. The size and phase composition were very variable without the use of poly(acrylic acid) and seeds. The use of high specific surface area calcite or vaterite powders in the presence of PAA in the potassium carbonate reactant gave control over the precipitated phase and influenced strongly the particle size distribution, whereas the use of PAA alone has no effect on precipitated products. Filtering these seed suspensions at 20 nm before use in the precipitation reaction still gave precipitated phase control and allowed further control over the particle size distribution. For calcite, particles with a median volume diameter (d_{v50}) of 500 nm and specific surface areas around 35 m^2/g were thus synthesized, indicative of nanosized primary particles of around 70 nm. Direct observation methods such as PCS or cryo-TEM did not succeed in detecting the presence of the sub-20-nm seeds. Consequently an indirect determination method was used, linking solubility measurement with solubility calculations via the Kelvin equation to give a seed size of around 8 nm with a number density of 2−16 seeds per μm^3. From the seed size and number density, primary particle sizes were computed assuming growth only on the nanosized seeds, and very good correlation with crystallite sizes from XRD line broadening and specific surface area measurements was found, particularly for the higher PAA concentrations used. The PAA concentration used in the production of the seeds seems to control the number density of seeds and consequently the final specific surface area of the precipitated powder. The variation of the particle morphology, from cuboid (low PAA concentrations) to ricelike ellipsoids, is thought to be linked to a ripening process, a discussion of which is outside the scope of the current study, but further work is being carried out and will be presented in a future paper.

Acknowledgment. The authors thank Danièle Laub (TEM), Sandrine Rousseau (ICP), and Corinne Daguenet for the practical synthesis work. This project was financially supported by the Swiss OFES (Office Fédéral de l'Education et de la Science), Contract No. OFES: 99.0449-1, in the frame of a European project in the 5th Framework, program GROWTH, Project SFTR No. G5RD-CT99-0123.

LA048525I